

Minimally disordered glasses

Karina González-López,¹ Eran Bouchbinder,² and Edan Lerner¹

¹*Institute for Theoretical Physics, University of Amsterdam, Science Park 904, Amsterdam, Netherlands*

²*Chemical and Biological Physics Department, Weizmann Institute of Science, Rehovot 76001, Israel*

Glasses, commonly formed by quickly cooling a liquid to avoid crystallization, and other amorphous materials pose great challenges due to their disordered nature. Understanding the range of variability of disorder is of prime importance, e.g. for discovering structure-properties relations. By rapidly compressing packings of grains, maximally disordered jammed states are known to emerge. In the other extreme, and in the context of glasses, it remains unknown if minimally disordered glasses exist or whether glasses feature continuously reduced disorder as they tumble down their complex potential energy landscape. Here we show, using extensive computer simulations of various glass-forming liquids, that there appears to be a lower bound on the degree of mesoscopic mechanical disorder, quantified by elastic constants fluctuations, of glasses formed by quenching a liquid. Furthermore, we show that the existence of minimally disordered glasses is intimately related to the existence of a mesoscopic glassy length scale. These results pose fundamental questions about the nature of glasses and have implications for their properties, such as sound attenuation and heat transport.

Glasses, and other amorphous solids such as granular materials, offer ever-growing opportunities for a huge range of technological applications and at the same time continue to pose some of the deepest scientific puzzles [1]. At the heart of both the technological applicability and basic scientific challenges resides the intrinsically non-equilibrium and disordered nature of these materials. When a glass is formed by quickly cooling a liquid below its melting point, it avoids crystallization and attains a non-equilibrium disordered structure. The latter is not unique, but rather depends on the preparation process itself and consequently glasses of the very same composition can feature widely different physical properties that depend on the spontaneously emerging state of disorder [2, 3]. Similar history dependence emerges when a packing of grains is compressed to form a granular solid [4, 5]. Quantifying glassy disorder, in particular understanding its range of variability and the corresponding variability in the emerging physical properties — such as elastic stiffness, plastic deformability, sound attenuation coefficient and heat transport — pose great challenges [6].

In the context of packings of grains, there exists the concept of maximally disordered (random) jammed states [4, 5], typically attained upon rapid compression. At the other extreme, and in the context of glasses formed by quenching a liquid, one can ask whether there exist minimally disordered glassy states. Naively, one would think as the glass tumbles down its complex potential energy landscape, the degree of disorder continuously reduces, at least until an “ideal glass state” is reached (if it exists [1]). Here we systematically address this fundamental question using extensive numerical simulations of various glass-forming liquids and recently developed concepts [6–8]. This combined computational-theoretical approach reveals for the first time the existence of minimally disordered glass states, which are not related to an ideal glass state, and rationalizes their physical origin.

Computer models of glass-forming liquids, examples of which are presented in Fig. 1, offer a unique platform for addressing basic questions in glass physics. One notable advantage of computer glasses is that their preparation process can be carefully controlled and quantified. In particular, the temperature T_p at which the glass falls out of equilibrium can be varied over a broad range, as explained and demonstrated in Fig. 1. Then various physical properties can be measured as a function of the glass’ thermal history, quantified by T_p , for a wide variety of computer glass-forming liquids. Another major advantage of computer glasses is that they allow detailed quantitative analysis of glassy disordered structures, down to the particle (atomistic) level, which is typically inaccessible to experiments.

These unique capabilities gave rise to some important recent progress. Most relevant here is the converging evidence for the existence of low-frequency glassy excitations [11–13], whose vibrational frequency ω follows a universal density of states $\mathcal{D}(\omega) = \mathcal{N}\omega^4/\omega_g^5$. Here \mathcal{N} is the number density of such glassy excitations and ω_g is their characteristic frequency, both dependent on T_p . These universal low-frequency glassy excitations qualitatively differ from low-frequency phonons, which follow Debye’s density of states, not only in their statistics, but also in their spatial properties; notably, while low-frequency phonons are spatially extended, low-frequency glassy excitations are quasilocalized, featuring a localization length ξ (cf. Fig. 1b) and power-law decaying fields on larger scales. It has been further demonstrated [7] that $\xi \sim \omega_g^{-1}$ (see also Appendix D), and that \mathcal{N} and ξ generally decrease with decreasing T_p , as illustrated in Fig. 1b.

The intrinsic glassy length scale ξ has also been shown to correspond to a crossover in the elastic response of glasses; on lengths smaller than ξ , elasticity is controlled by glassy disorder, while on larger lengths, continuum elasticity is recovered [6, 14]. Yet, in itself, ξ does not

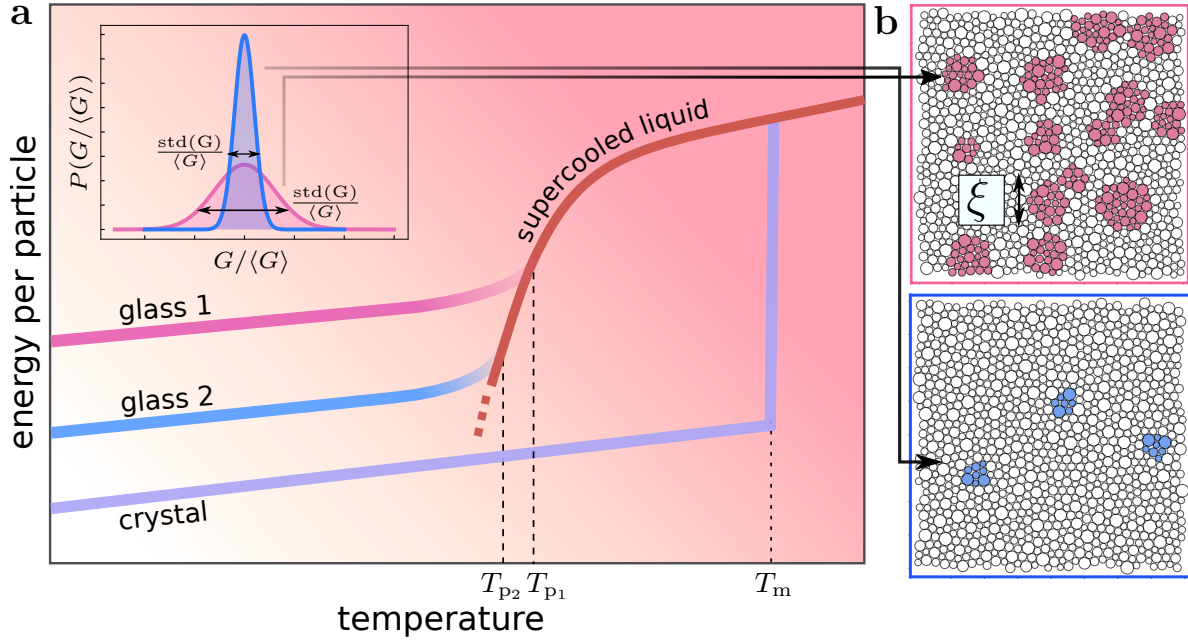


FIG. 1. Quantifying glass preparation history, mechanical disorder and intrinsic length scale. **a**, The potential energy per particle of a glass-forming liquid is schematically plotted against its temperature. At high temperatures, above the melting temperature T_m , the material is in an equilibrium liquid state. If the liquid is then cooled sufficiently slowly, it crystallizes at T_m (purple line). If, on the other hand, cooling is sufficiently fast, crystallization at the melting point is avoided and the supercooled liquid regime is entered (red line). Recent developments in computer glass techniques allow to follow the supercooled equilibrium line to unprecedented depth, presumably even deeper than laboratory glasses [9]. At each temperature along the supercooled equilibrium line, to be denoted hereafter by T_p , a glass can be formed by instantaneously cooling the liquid to a mechanically stable state at zero temperature, a process illustrated by the two lines branching off the supercooled equilibrium line (pink line, corresponding to T_{p_1} , and blue line, corresponding to $T_{p_2} < T_{p_1}$). T_p in this well-controlled procedure can be regarded as the temperature at which the glass falls out of equilibrium. **(inset)** Schematic distributions of the shear modulus G , $P(G/\langle G \rangle)$ ($\langle G \rangle$ is the average of the distribution), corresponding to the two T_p values specified on the main panel. The relative width of the distribution, $\text{std}(G)/\langle G \rangle$ ($\text{std}(G)$ is G 's standard deviation), allows to define the dimensionless measure of mechanical disorder $\chi \propto \text{std}(G)/\langle G \rangle$, see text for details. With decreasing T_p , $\text{std}(G)/\langle G \rangle$ tends to decrease, as the illustration indicates. The main question posed in the paper is whether $\chi \propto \text{std}(G)/\langle G \rangle$ saturates at a lower bound at some T_p , prior to the hypothetical intersection of the supercooled (red) line with the crystalline (purple) line. **b**, Snapshots of two glasses generated using a computer glass-forming liquid model [10]. The upper (lower) panel corresponds to a glass generated at T_{p_1} (T_{p_2}), where soft quasilocalized modes are illustrated by pink (blue) particles. It is observed that with decreasing T_p , the number of soft quasilocalized modes (denoted by \mathcal{N} in the text, see details therein) decreases and their typical size, marked by ξ , decreases as well.

immediately provide a measure of glassy disorder. While many quantifiers of glassy disorder have been proposed and studied in the literature, we focus here on *mesoscopic mechanical disorder* as quantified by the relative fluctuations of the shear modulus G . The latter can be computed by generating many realizations of a glass of N particles under exactly the same preparation process, constructing the sample-to-sample probability distribution function $p(G/\langle G \rangle)$ — as illustrated in the inset of Fig. 1a — and then calculating $\chi \equiv \delta G/\langle G \rangle$, where $\langle \bullet \rangle$ stands for an ensemble average and $\delta G \equiv \sqrt{N\langle (G - \langle G \rangle)^2 \rangle}$. χ , which provides a dimensionless measure of mechanical disorder [15], has been very recently shown to control the attenuation of long-wavelength waves in glasses [16] and hence to be also related to heat transport in these materials. Consequently, χ is expected to play a major role in establishing thermo-mechanical structure-properties relations in glasses.

To address the possible existence of minimally disordered glass states, we employ 9 different computer glass-forming models (see Appendix A for details), featuring a wide variety of interparticle potentials — from purely repulsive to strongly attractive —, and different compositions — from binary mixtures to broadly polydispersed. For each model, we create large ensembles of independent athermal ($T = 0$) glassy samples parameterized by the equilibrium parent temperature T_p from which they were rapidly quenched (cf. Fig. 1a); T_p was varied from high temperature liquid states to deeply supercooled states. In Fig. 2, we plot χ as a function of the depth of supercooling of our glasses' ancestral liquid states, quantified by T_p (lower x -axis). χ generically plateaus at large T_p , where the plateau levels vary over a factor of roughly 4 between the employed glasses, underlying their wide diversity. As T_p decreases, χ appears to converge to a master envelope curve that features a *lower bound* χ_0 . That is, despite the large variability in the em-

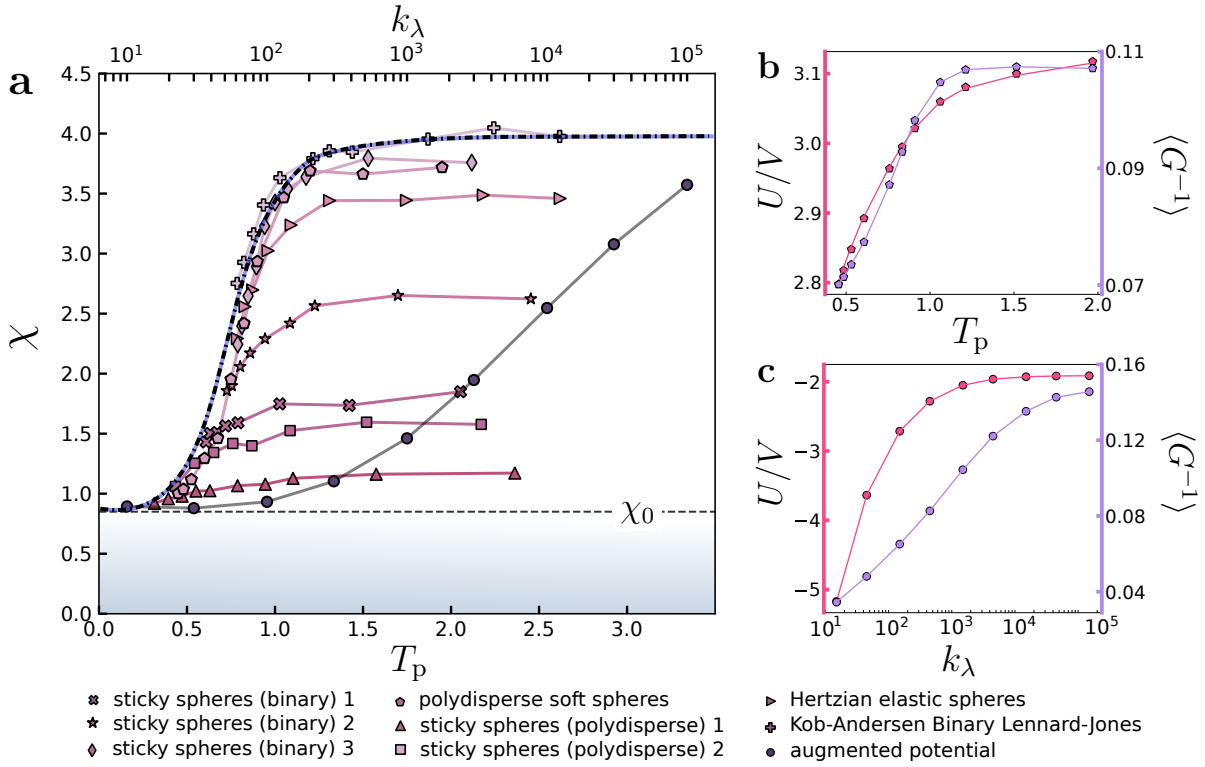


FIG. 2. The existence of minimally disordered glassy states across a broad range of computer glasses. **a**, The dimensionless quantifier of mechanical disorder χ is extracted for 9 different glass models (see legend and Appendix A); in 8 of these models, χ depends on T_p , as described in Fig. 1. T_p is expressed in terms of a model-dependent crossover temperature [17], see also Appendix B. It is observed that the $\chi(T_p)$ curves of the different models converge to a master envelope curve marked by a dash-dotted guide to the eye, which appears to be bounded from below. The 9th model — the so-called augmented potential model — corresponds to a computer glass that is not formed by quenching a liquid. In particular, it is a computer glass model in which particle radii were included as additional degrees of freedom, yielding amorphous states with very large variability in mechanical stability [18]. This has been achieved by varying a tunable parameter k_λ , which controls the relative importance of the radii degrees of freedom, where for $k_\lambda \rightarrow \infty$ these degrees of freedom are entirely frozen, and a generic computer glass is recovered. In the figure, we plot χ as a function of k_λ (logarithmic scale, upper x-axis). It is observed that, remarkably, while the functional form of $\chi(k_\lambda)$ is quite different from the master curve corresponding to thermally-annealed glasses, it approaches the very same minimal χ value, lending further support to the generality of the existence of minimally disordered glasses. The existence of a lower bound on χ appears to be further supported by reports on a frustration-induced amorphization transition of crystalline structures into highly-disordered glasses [19], which seems to be accompanied by an inaccessible range of degree of elastic fluctuations. Note that χ is related to the ‘disorder parameter’ introduced in [20, 21], under certain conditions [16]. **b**, The potential energy density U/V (left y-axis) and the shear compliance $\langle G^{-1} \rangle$ for the polydisperse soft spheres model, as a function of T_p , over the same range shown in panel a. It is observed that both quantities continuously decrease with decreasing T_p , while $\chi(T_p)$ saturates at its lowest bound χ_0 . **c**, The same as panel b, but for the augmented potential model, where T_p is replaced by k_λ . It is again observed that both U/V and $\langle G^{-1} \rangle$ continuously decrease with decreasing k_λ , most importantly in the very same region where $\chi(k_\lambda)$ in panel a appears to be fully saturated at the lower bound χ_0 .

ployed computer glass-forming liquids, there appears to be a minimal level of mechanical disorder χ — marked by the horizontal dashed line $\chi = \chi_0$ — that a glass can attain through varying T_p , i.e. by thermal annealing.

It is crucial to stress that the existence of these minimally disordered glass states does not appear to be accompanied by any clear transition or crossover inside the glass phase, and in particular these states appear to have nothing to do with any hypothetical “ideal glass state” [1]. This important point is highlighted in Fig. 2b, where it is shown that the potential energy density and the shear compliance of a glass continue to evolve with decreasing T_p , while $\chi(T_p)$ saturates at its lowest bound

χ_0 . Which physical observables do vary in a glass below the aforementioned saturation of χ ? It was previously shown [7] that, for low T_p ’s, the number density \mathcal{N} of soft quasilocalized excitations follows a Boltzmann-like law with T_p . This strong dependence on T_p is expected to persist below the saturation of χ , implying that below some T_p , the population of soft quasilocalized excitations is too small to affect χ .

The emergence of minimally disordered glass states is demonstrated in Fig. 2 for glasses formed by quenching a liquid (lower x-axis), which is indeed the most prevalent glass preparation procedure. Yet, glasses can be also formed by other procedures, for example by vapor

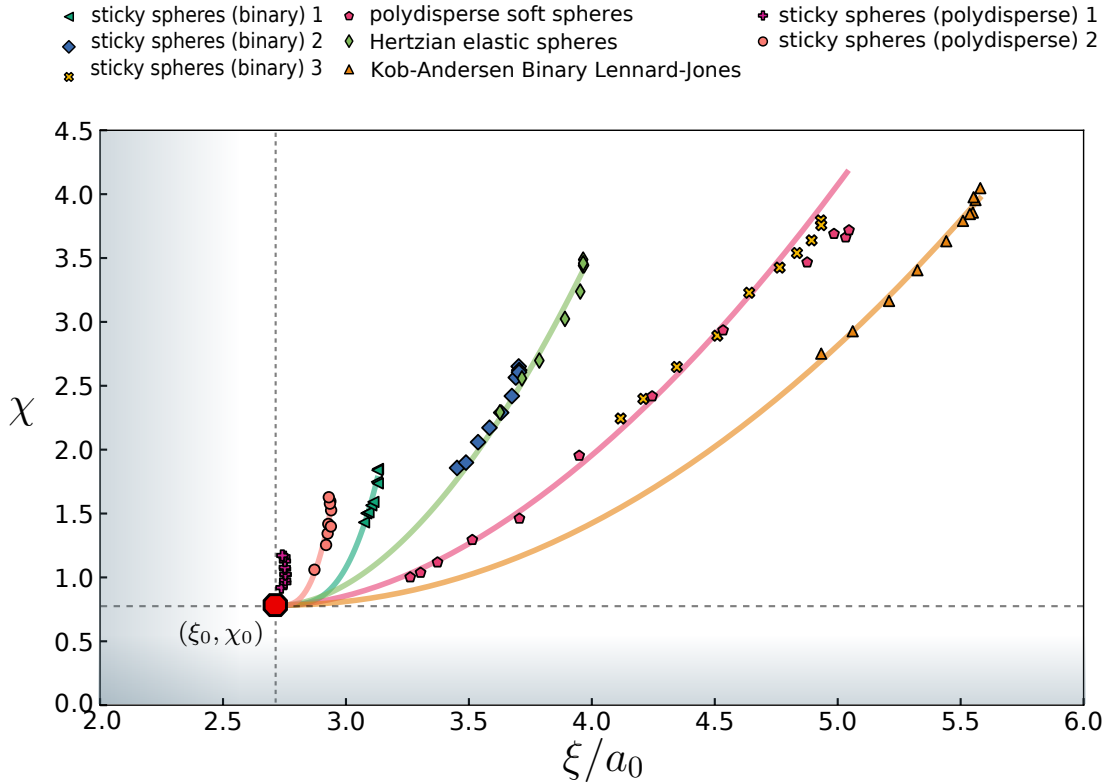


FIG. 3. **The degree of mesoscopic mechanical disorder is related to a mesoscopic glassy length scale.** The dimensionless measure of mesoscopic mechanical disorder χ , previously shown in Fig. 2 for 8 computer glass-forming liquids as a function of T_p , is plotted against the mesoscopic glassy length scale ξ (see Appendix D and text for additional details). The data are parameterized by T_p , i.e. we focus here on glasses formed by quenching a liquid, and ξ is normalized by a characteristic interparticle distance a_0 . On each data set, corresponding to a different computer glass-forming liquid (see legend), a solid curve is superimposed as a guide to the eye. The resulting curves suggest that the existence of a minimum degree of mechanical disorder χ_0 is intimately related to a corresponding minimum of ξ , i.e. ξ_0 , of a few interparticle distances. Furthermore, the observations that none of the $\chi(\xi)$ for the different computer glass-forming liquids intersect and that some curves of significantly different liquids (e.g. ‘sticky spheres (binary) 2’ and ‘Hertzian elastic spheres’, see legend) practically overlap, suggest that $d\chi/d\xi$ is a unique function of ξ and χ , independently of the specific glass-forming liquid.

deposition[22]. One can then ask whether such glasses, i.e. glasses not formed by quenching a liquid, also feature a lower bound on χ and if so, whether it is identical to χ_0 found in Fig. 2. While we do not systematically address this question here, the powerful and flexible tools offered by available computer glass models can already start shedding light on it. In Fig. 2 (upper x -axis), we show that a computer glass that is not formed by quenching a liquid nevertheless approaches the very same minimal χ value, lending further support to the generality of the existence of minimally disordered glasses. The degree of universality of these observations should be further addressed in future investigations.

The results presented in Fig. 2 strongly indicate that minimally disordered glass states exist, i.e. that glasses formed by quenching a liquid (and possibly also glasses formed through other physical procedures) cannot feature a degree of mechanical disorder — as quantified by χ — smaller than a certain finite lower bound χ_0 . What is the physical origin of such a lower bound? To ad-

dress this question, we consider the glassy length scale ξ , introduced above in the context of low-frequency quasilocalized glassy excitations, and its possible relation to the mechanical disorder measure χ . First, let us stress — as explained above — that while ξ characterizes the spatial localization of low-frequency quasilocalized glassy excitations, it is a more general glassy length scale that characterizes the elastic response of glasses, independently of the existence of these excitations. In particular, ξ marks the crossover from disordered-controlled microscopic elasticity on small lengths to conventional continuum elasticity on large lengths [14, 23]. Since micromechanical fluctuations appear to be correlated on a spatial scale ξ , it is expected that the same correlation length also characterizes the spatial fluctuations of coarse-grained fields of elastic constants.

The identification of ξ with the correlation length of elastic constants fluctuations implies, in turn, that the value of χ should depend on ξ . The idea that χ systematically depends on ξ , i.e. that a function $\chi(\xi)$ exists

for a given glass when T_p is varied, might rationalize the existence of a lower bound on χ . As it is known that both χ and ξ decrease with decreasing T_p [7, 24], the hypothesized relation $\chi(\xi)$ implies that a minimal value of χ is related to a minimal value of ξ . The existence of the latter is unavoidable, simply because ξ is bounded from below by the discreteness of the material, i.e. it cannot be smaller than a few interparticle distances. Consequently, we hypothesize that $\chi(\xi)$ — for a given glass and as T_p is varied — is a well-defined monotonically decreasing function of decreasing ξ , which therefore also reveals a minimal ξ , denoted hereafter by ξ_0 . Moreover, we expect that if this picture is valid, then while different glasses may give rise to different $\chi(\xi)$ curves, all of these would approximately feature the same ξ_0 , corresponding to $\chi_0 = \chi(\xi_0)$.

This physical picture is tested in Fig. 3, where χ is plotted against ξ (see Appendices C,D for details), parameterized by T_p , for the broad variety of computer glass models shown in Fig. 2. As rationalized above, a family of monotonically decreasing functions $\chi(\xi)$ emerges, each of which appears to extrapolate (continuous lines) to *the same* point (ξ_0, χ_0) in the ξ - χ plane, marked by the red button. One can then hypothesize that the local variation of χ with ξ is determined by a unique function $\mathcal{F}(\xi, \chi)$, i.e. $d\chi/d\xi = \mathcal{F}(\xi, \chi)$. This intriguing hypothesis implies that different $\chi(\xi)$ curves do not intersect and consequently that glasses that share a single (ξ, χ) point, feature the very same $\chi(\xi)$ curve. These properties are strongly supported by the results in Fig. 3. A first-principle understanding of the function $\mathcal{F}(\xi, \chi)$ is a burning problem to be addressed in future work.

The existence of a lower bound on the mesoscopic mechanical disorder of glasses may raise the question about the possible existence of an upper bound. The results presented in Fig. 2a indicate that for glasses formed by quenching a liquid such an upper bound may exist, but that it is clearly not universal, i.e. it depends on the specific glass under consideration. As mentioned above, maximally disordered jammed states are known to exist for rapidly compressed packings of stiff grains. The degree of mechanical disorder of these grain packings, which constitute a class of amorphous solids different from glasses formed by quenching a liquid, can also be quantified by χ . In this case, χ is expected [25] to be related to the Poisson's ratio ν of the packing according to $\chi \sim 1/(1 - 2\nu)$ in the limit of very stiff grains, where ν is close to its limiting value $1/2$. In this limit, χ diverges, i.e. there exists no upper bound on the degree of mechanical disorder for grain packings.

In this work, we proposed a physically transparent way to quantify the degree of mesoscopic mechanical disorder featured by structural glasses quenched from a melt. Intriguingly, we find evidence indicating that the dimensionless disorder quantifier χ — that captures relative shear modulus fluctuations and generally decreases under thermal annealing — is bounded from below. We ra-

tionalize this bound by establishing a link between χ and a mesoscopic glassy length that characterizes the spatial extent of the elastic response of glasses to local perturbations [7], which cannot fall below a few interparticle distances. Our analyses constitute a major step towards establishing a unifying framework to organize structural glasses into different classes according to their featured degree of mechanical disorder, and its potential variability under thermal annealing.

ACKNOWLEDGMENTS

We thank Geert Kapteijns, David Richard, Corrado Rainone, Talya Vaknin, Avraham Moriel, and Gustavo Düring for their comments on the manuscript. We greatly benefited from discussions with Gustavo Düring, David Richard, and Massimo Pica Ciamarra, who are warmly acknowledged. We highlight in particular Geert Kapteijns's contribution to resolving the χ - ν relation. E. B. acknowledges support from the Minerva Foundation with funding from the Federal German Ministry for Education and Research, the Ben May Center for Chemical Theory and Computation, and the Harold Perlman Family. E. L. acknowledges support from the NWO (Vidi grant no. 680-47-554/3259).

Appendix A: Computer glasses

In our work we presented results from extensive simulations and analyses of 9 different computer models of glass-forming liquids. Here we provide brief descriptions of the models listed in the legends of Figs. 2 and 3 of the main text. We specify the system sizes N employed, and the number of independent glass samples n that constitute each ensemble for the estimations of χ as seen in the main text. All of the models are studied in three-dimensions (3D) using a cubic box of fixed volume $V = L^3$ with standard periodic boundary conditions [26]. Liquids were equilibrated at each parent temperature using molecular dynamics, unless stated otherwise. After equilibration, each system is instantaneously quenched to a local minimum of the potential energy using a conventional minimization algorithm, to obtain an athermal glasses.

For each model, a crossover temperature T_x is estimated following the approach presented in Ref. [17], which is briefly explained in Sect. B. The estimated values of T_x — expressed in terms of each model's individual simulation units — are reported in Table I. In addition, we refer to relevant literature where further information about the models and protocols used to prepare our ensembles of athermal glasses can be found.

TABLE I. Crossover temperatures T_x — expressed in terms of models’ respective *simulational* units — as estimated for the computer glass models employed in this work, following the approach presented in [17].

computer glass model	T_x
Sticky spheres (binary) 1	1.26
Sticky spheres (binary) 2	1.06
Sticky spheres (binary) 3	0.85
Sticky spheres (polydisperse) 1	1.27
Sticky spheres (polydisperse) 2	0.921
Polydisperse soft spheres	0.66
Hertzian elastic spheres	0.0023
Kob-Andersen binary Lennard-Jones	0.535

1. Sticky spheres (binary)

This is a 50:50 binary mixture of ‘small’ and ‘large’ particles that interact pairwise via a piece-wise Lennard-Jones-like potential, introduced first in [27], and studied extensively in Refs. [6, 8, 28, 29]. In this model, the strength of attractions between the glass’s constituent particles can be readily tuned by varying the interaction cutoff-length r_c . In our work we employ three different cutoff-lengths: $r_c = 1.2, 1.3, 1.5$ enumerated in Figs. 2 and 3 of the main text as ‘1,2,3’, respectively. To estimate the dimensionless quantifier of mechanical disorder χ , we used $n=9200$ independent glasses of $N=3000$ particles for $r_c = 1.2, 1.3$ and $n = 3000$ independent glasses of $N=10000$ particles for $r_c = 1.5$, for each parent temperature, in order to minimize finite size effects, as discussed further below. The number density is fixed to $N/V = 0.60\lambda^{-3}$ for all of the ‘1,2,3’ ($r_c = 1.2, 1.3, 1.5$) variants of the model, where λ denotes the effective size of the ‘small’ species. For further information about the model and glass preparation protocol see Ref. [8].

2. Sticky spheres (polydisperse)

In this model pairs of particles interact via the same pairwise potential as in the ‘Sticky sphere (binary)’ model discussed above, in which the cutoff length r_c serves as the key control parameter. We follow Ref. [9] and draw each particle’s effective size λ_i from a distribution $p(\lambda) \sim \lambda^{-3}$, between $\lambda_{\min} = 1.0\lambda$ and $\lambda_{\max} = 2.22\lambda$, where λ is the simulation units of length. We study two variants of this model, that differ in their respective cutoff-lengths: $r_c = 1.1$, referred to as ‘sticky spheres (polydisperse) 1’ in the main text, and $r_c = 1.2$, referred to as ‘sticky spheres (polydisperse) 2’ in the main text. The models’ polydispersity is used to exploit the power of the Swap Monte Carlo Method [9] to obtain deeply supercooled equilibrium states. Finite-size effects induced by random particle-sizes are dealt with as explained in [24].

We choose the number density $N/V = 0.40\lambda^{-3}$ such that the high parent-temperature glasses’ pressure to bulk modulus ratio $p/K \approx 0.05$. We employed systems of $N = 2000$ particles, independent of T_p for both model variants. χ was measured using at least 8900 independent glasses for all T_p ’s with $r_c = 1.1$, and $n = 11100$ glasses for all T_p ’s using $r_c = 1.2$.

3. Polydisperse soft spheres

This model consists of particles of random effective sizes that are distributed and chosen in the same way as done for the Sticky spheres (polydisperse) model described above. Pairs of particles interact via an inverse-power-law (IPL) pairwise potential $\varphi_{\text{IPL}} \sim r^{-10}$ (r is the interparticle separation), truncated and smoothed as explained in e.g. Ref. [24]. Equilibrium states were obtaining using the Swap Monte Carlo method[9], which allows one to obtain very deeply supercooled states. For systems with rescaled parent temperature $T_p \geq 0.59T_x$ we generated $n=2000$ glasses per T_p , of $N=16000$ particles, however due to the viscous slow-down of dynamics intrinsic to glass-formers, we generated $n=10000$ uncorrelated glasses of $N=2000$ for $T_p < 0.59T_x$. The number density was fixed at $N/V = 0.58\lambda^{-3}$ for all systems. This model was studied extensively in [7, 24] where further details can be found, including an explanation about how the polydispersity is chosen, and how disorder-realization-induced finite-size effects are handled.

4. Hertzian elastic spheres

The Hertzian elastic spheres model is a 50:50 binary mixture of small and large soft, linear-elastic spheres interacting via the Hertzian interaction law [30]. We simulate $n=10000$ systems of $N=4000$ particles for all T_p ’s at a fixed number density $N/V = 0.9386\lambda^{-3}$, where λ denotes the diameter of the small particles. For this number density, and for glasses of high T_p ’s, the typical ratio of the pressure to bulk modulus is $p/K \approx 0.17$. Information about the parameters employed and further details can be found in Ref. [13].

5. Kob-Andersen binary Lennard-Jones

Perhaps the most thoroughly studied computer glass former is the Kob-Andersen binary Lennard-Jones model [31]. This canonical glass former is a binary mixture of 80% type A (‘large’) particles, to 20% type B (‘small’) particles, which interact via the standard 12-6 Lennard-Jones potential. The potential was truncated smoothly up to the first derivative, following Ref. [32]. The system size chosen is $N = 3000$ and the number den-

sity is set to $N/V = 1.2$ in all ensembles. A minimum of $n = 8970$ independent glasses per T_p were used to estimate χ .

6. Augmented potential glasses

In contrast with all the above described glass-forming models, the ‘Augmented potential’ model allows generating computer glasses that are not formed by the conventional route of quenching a liquid. In this model, on top of the three usual degrees of freedom per particle, particles’ effective sizes are allowed to fluctuate at some energetic cost. The latter is controlled by a stiffness k_λ ; as $k_\lambda \rightarrow \infty$, the particles’ sizes are frozen, and the model reduces to a conventional computer glass model. We use the glasses generated in Ref. [18], where it was shown that k_λ plays a crucial role in obtaining ultra-stable glasses by systematically varying k_λ between 10^1 to 10^5 . We chose a system size of $N = 4000$ particles for all k_λ ’s, and number densities: $N/V = 1.2660, 0.8945, 0.6765, 0.5801, 0.5332, 0.5166, 0.5102, 0.5082, 0.5075$, expressed in terms of λ^{-3} (see Ref. [18] for definition), for $k_\lambda = 10, 30, 100, 300, 1000, 3000, 10000, 30000, 100000, 300000$, respectively. The number of independent samples used to estimate χ was $n = 42,000$ for all k_λ ’s except for $k_\lambda = 30$, where $n = 10000$.

Appendix B: Crossover temperature

We follow [17] and extract a crossover temperature for a given computer liquid as follows: we consider a large ensemble of equilibrium liquid states at temperature T . For each such state, we follow steepest-descent dynamics and record the mean and standard deviation of particles’ squared displacements $\overline{\delta r^2}$ between the initial, equilibrium state, to the inherent state that is inevitably reached [33]. The ratio of the aforementioned standard deviation and mean of the squared displacements forms a dimensionless number, that is a nonmonotonic function of the equilibrium temperature T [17]. The temperature at which this function assumes a maximum is defined as the crossover temperature, with respect to which all temperatures in our work were expressed.

Appendix C: Estimating the dimensionless quantifier χ

Estimating the dimensionless quantifier χ of sample-to-sample shear modulus fluctuations is oftentimes challenging due to strong finite size effects, as explained at length in Refs. [8, 16]. We calculated the shear modulus G of any given athermal glass following the standard framework [34]. In Fig. 4 we demonstrate that as lower

parent temperatures T_p are considered, finite-size effects weaken, due to the associated decrease of ξ [7, 23]. To avoid these finite size effects, for some models we employ relatively large system sizes (typically of $\mathcal{O}(10^4)$ particles) for high parent temperatures T_p .

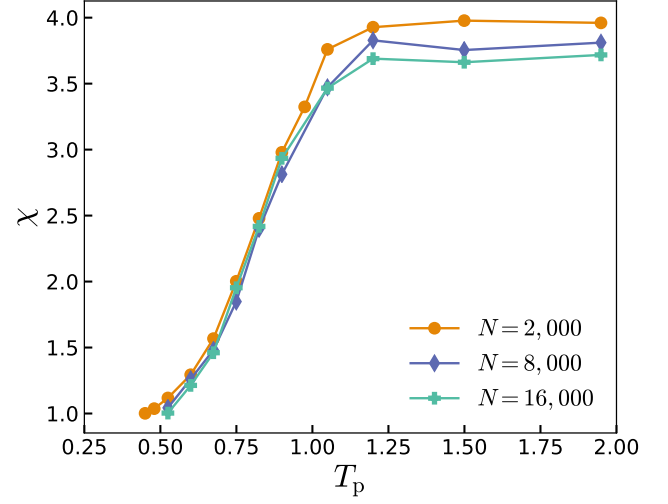


FIG. 4. **Finite size effects in χ are tamed at low T_p .** χ is a dimensionless quantifier of relative shear modulus fluctuations. Here we estimate χ following the scheme put forward in [6], and plot it against the rescaled parent temperature T_p/T_x for the Polydisperse soft spheres model described above. We observe that finite-size effects are insignificant for small glasses at low temperatures, and become more relevant at high parent temperatures, motivating our choices of system sizes throughout our work.

It has been shown [16] that the sample-to-sample variance of G displays strong finite-size effects; we handled the latter using a Jackknife-like method as explained in detail in [6], using the same single dimensionless parameter as used there.

Appendix D: Mesoscopic length estimation

Structural glasses are known to generically host a population of non-phononic, quasilocalized low-frequency modes [11–13]. These modes have been shown to feature a disordered core — of size ξ — and to be decorated by Eshelby-like algebraic decaying fields [11], which is why these modes are often referred to as *soft quasilocalized-modes* (QLMs). Following Refs. [7, 8, 35], we estimate QLMs’ core size as follows: denoting by $\mathbf{d}^{(ij)}$ a force dipole applied to the i, j pair, the linear displacement response of the system to such a force reads

$$\mathbf{u}^{(ij)} = \mathbf{M}^{-1} \cdot \mathbf{d}^{(ij)}, \quad (D1)$$

where we have defined the Hessian $\mathbf{M} = \frac{\partial^2 U}{\partial \mathbf{x} \partial \mathbf{x}}$ of the potential energy $U(\mathbf{x})$ that depends on particle coordinates

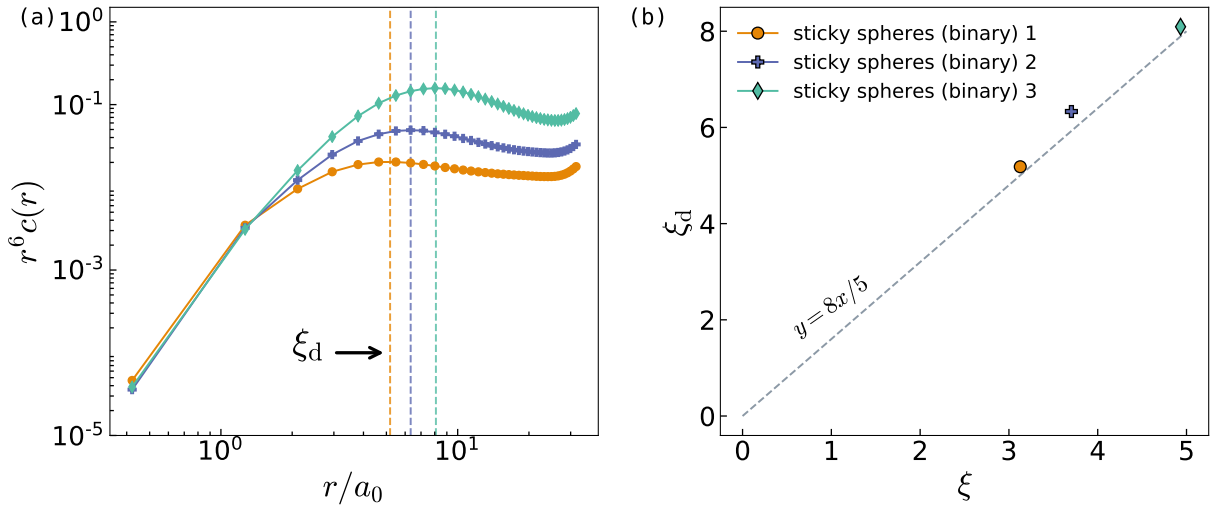


FIG. 5. **Extracting the glassy length scale ξ .** In our work we estimate the glassy length ξ via Eq. (D4), as explained in the text. To demonstrate the validity Eq. (D4) we show in panel (a) the averaged decay profiles $c(r)$ (see e.g. [7] for $c(r)$'s definition) of linear displacement responses to local dipole forces (for the 3 glass forming model as indicated by the legend), factored by r^6 , and plotted against r/a_0 , where r is the distance from the applied local force dipole, and a_0 is a characteristic interparticle distance. The crossover length ξ_d — marked by the (color-coded, see legend) dashed vertical lines — is defined as the maximum of the products $r^6 c(r)$ found by fitting a cubic polynomial to the peak region (see also Ref.[6]). We compare between the two lengths ξ and ξ_d in panel (b), where they are plotted against each other.

x. The frequency $\omega_g^{(ij)}$ associated with the displacement response $\mathbf{u}^{(ij)}$ is given by [7, 35]

$$\omega_g^{(ij)} \equiv \sqrt{\frac{\mathbf{u}^{(ij)} \cdot \mathbf{M} \cdot \mathbf{u}^{(ij)}}{\mathbf{u}^{(ij)} \cdot \mathbf{u}^{(ij)}}} = \sqrt{\frac{\mathbf{d}^{(ij)} \cdot \mathbf{M}^{-1} \cdot \mathbf{d}^{(ij)}}{\mathbf{d}^{(ij)} \cdot \mathbf{M}^{-2} \cdot \mathbf{d}^{(ij)}}}, \quad (\text{D2})$$

The characteristic frequency ω_g is obtained by averaging $\omega_g^{(ij)}$ over interacting-pairs and glass samples, i.e.,

$$\omega_g \equiv \langle \omega_g^{(ij)} \rangle_{ij}. \quad (\text{D3})$$

Finally, we use the relation put forward in [7] to estimate the QLMs' core-size ξ (illustrated in Fig. 1 of the main

text), as:

$$\xi = 2\pi c_s / \omega_g, \quad (\text{D4})$$

where $c_s = \sqrt{G/\rho}$ is the zero-frequency shear wave speed, G is the shear modulus, and ρ denotes the mass density.

As explained in the main text, the glassy length ξ has also been shown to mark the crossover between glassy disorder-controlled elasticity on small lengths of order ξ , to continuum linear elasticity on lengths larger than ξ [14]. Thus, if large glasses (of about 100K particles or larger) are available, it is also possible to estimate ξ by considering the average decay profiles $c(r) \propto \langle \mathbf{u}^{(ij)} \cdot \mathbf{d}^{(k\ell)} \rangle_{r_{ij}, k\ell \approx r}$ extracted from responses $\mathbf{u}^{(ij)}$, see Refs. [7, 23] for further details. In particular, $c(r) \sim r^{-2d}$ in d spatial dimensions is observed [7, 14, 23]. Examples of factored decay profiles $r^6 c(r)$, the extracted length ξ_d , and their comparison with ξ as estimated via Eq. (D4), are shown in Fig. 5.

- [1] P. G. Debenedetti and F. H. Stillinger, Supercooled liquids and the glass transition, *Nature* **410**, 259 (2001).
- [2] J. Ketkaew, W. Chen, H. Wang, A. Datye, M. Fan, G. Pereira, U. D. Schwarz, Z. Liu, R. Yamada, W. Dmowski, M. D. Shattuck, C. S. O'Hern, T. Egami, E. Bouchbinder, and J. Schroers, Mechanical glass transition revealed by the fracture toughness of metallic glasses, *Nature Communications* **9**, 3271 (2018).
- [3] B. Sun, Y. Hu, D. Wang, Z. Zhu, P. Wen, W. Wang, C. Liu, and Y. Yang, Correlation between local elastic

- heterogeneities and overall elastic properties in metallic glasses, *Acta Mater.* **121**, 266 (2016).
- [4] N. Epstein and M. J. Young, Random loose packing of binary mixtures of spheres, *Nature* **196**, 885 (1962).
- [5] L. E. Silbert, Jamming of frictional spheres and random loose packing, *Soft Matter* **6**, 2918 (2010).
- [6] K. González-López, Y. Zheng, M. Shivam, M. Pica Ciamarra, and E. Lerner, Mechanical disorder of sticky-sphere glasses. i. effect of attractive interactions, *arXiv preprint arXiv:2008.12011* (2020).

[7] C. Rainone, E. Bouchbinder, and E. Lerner, Pinching a glass reveals key properties of its soft spots, *Proc. Natl. Acad. Sci. U.S.A.* **117**, 5228 (2020).

[8] K. González-López, M. Shivam, Y. Zheng, M. Pica Ciamarra, and E. Lerner, Mechanical disorder of sticky-sphere glasses. ii. thermo-mechanical inannealability, *arXiv preprint arXiv:2009.08238* (2020).

[9] A. Ninarello, L. Berthier, and D. Coslovich, Models and algorithms for the next generation of glass transition studies, *Phys. Rev. X* **7**, 021039 (2017).

[10] A. Moriel, G. Kapteijns, C. Rainone, J. Zylberg, E. Lerner, and E. Bouchbinder, Wave attenuation in glasses: Rayleigh and generalized-rayleigh scattering scaling, *J. Chem. Phys.* **151**, 104503 (2019).

[11] E. Lerner, G. Düring, and E. Bouchbinder, Statistics and properties of low-frequency vibrational modes in structural glasses, *Phys. Rev. Lett.* **117**, 035501 (2016).

[12] G. Kapteijns, E. Bouchbinder, and E. Lerner, Universal nonphononic density of states in 2d, 3d, and 4d glasses, *Phys. Rev. Lett.* **121**, 055501 (2018).

[13] D. Richard, K. González-López, G. Kapteijns, R. Pater, T. Vaknin, E. Bouchbinder, and E. Lerner, Universality of the nonphononic vibrational spectrum across different classes of computer glasses, *Phys. Rev. Lett.* **125**, 085502 (2020).

[14] E. Lerner, E. DeGiuli, G. During, and M. Wyart, Breakdown of continuum elasticity in amorphous solids, *Soft Matter* **10**, 5085 (2014).

[15] Under certain assumptions, discussed at length in [16], $\chi^2 \sim \gamma$, where γ is Schirmacher's 'disorder parameter' [20, 21].

[16] G. Kapteijns, D. Richard, E. Bouchbinder, and E. Lerner, Elastic moduli fluctuations predict wave attenuation rates in glasses, *arXiv preprint arXiv:2008.08337* (2020).

[17] K. González-López and E. Lerner, An energy-landscape-based temperature scale in liquids, *arXiv preprint arXiv:2010.07153* (2020).

[18] G. Kapteijns, W. Ji, C. Brito, M. Wyart, and E. Lerner, Fast generation of ultrastable computer glasses by minimization of an augmented potential energy, *Phys. Rev. E* **99**, 012106 (2019).

[19] H. Mizuno, S. Mossa, and J.-L. Barrat, Acoustic excitations and elastic heterogeneities in disordered solids, *Proc. Natl. Acad. Sci. U.S.A.* **111**, 11949 (2014).

[20] W. Schirmacher, G. Ruocco, and T. Scopigno, Acoustic attenuation in glasses and its relation with the boson peak, *Phys. Rev. Lett.* **98**, 025501 (2007).

[21] A. Marruzzo, W. Schirmacher, A. Fratalocchi, and G. Ruocco, Heterogeneous shear elasticity of glasses: the origin of the boson peak, *Sci. Rep.* **3**, 1407 EP (2013).

[22] M. D. Ediger, Perspective: Highly stable vapor-deposited glasses, *J. Chem. Phys.* **147**, 210901 (2017).

[23] E. Lerner, Finite-size effects in the nonphononic density of states in computer glasses, *Phys. Rev. E* **101**, 032120 (2020).

[24] E. Lerner, Mechanical properties of simple computer glasses, *J. Non-Cryst. Solids* **522**, 119570 (2019).

[25] C. P. Goodrich, S. Dagois-Bohy, B. P. Tighe, M. van Hecke, A. J. Liu, and S. R. Nagel, Jamming in finite systems: Stability, anisotropy, fluctuations, and scaling, *Phys. Rev. E* **90**, 022138 (2014).

[26] M. P. Allen and D. J. Tildesley, *Computer simulation of liquids* (Oxford university press, 1989).

[27] S. Karmakar, E. Lerner, I. Procaccia, and J. Zylberg, Effect of the interparticle potential on the yield stress of amorphous solids, *Phys. Rev. E* **83**, 046106 (2011).

[28] O. Dauchot, S. Karmakar, I. Procaccia, and J. Zylberg, Athermal brittle-to-ductile transition in amorphous solids, *Phys. Rev. E* **84**, 046105 (2011).

[29] J. Chattoraj and M. P. Ciamarra, Role of attractive forces in the relaxation dynamics of supercooled liquids, *Phys. Rev. Lett.* **124**, 028001 (2020).

[30] L. D. Landau and E. M. Lifshits, *Theory of Elasticity* (Pergamon Press, 1964).

[31] W. Kob and H. C. Andersen, Testing mode-coupling theory for a supercooled binary lennard-jones mixture i: The van hove correlation function, *Phys. Rev. E* **51**, 4626 (1995).

[32] P. Leishangthem, A. D. S. Parmar, and S. Sastry, The yielding transition in amorphous solids under oscillatory shear deformation, *Nat. Commun.* **8**, 14653 (2017).

[33] S. Sastry, P. G. Debenedetti, and F. H. Stillinger, Signatures of distinct dynamical regimes in the energy landscape of a glass-forming liquid, *Nature* **393**, 554 (1998).

[34] J. F. Lutsko, Generalized expressions for the calculation of elastic constants by computer simulation, *J. Appl. Phys.* **65**, 2991 (1989).

[35] E. Lerner and E. Bouchbinder, A characteristic energy scale in glasses, *J. Chem. Phys.* **148**, 214502 (2018).